

0.3% with the values deduced using the magnetic spectrometer.

¹⁰The material in the path of the recoil proton, contributing to multiple scattering (ms), consisted of 2.9×10^{-3} radiation lengths (rl) of material perpendicular to the π beam (1.5×10^{-3} rl of liquid H_2 plus 1.4×10^{-3} rl of other material) plus 0.8×10^{-3} rl perpendicular to the proton line of flight. For 20% of the events, an additional average of 5.6×10^{-3} rl of Cu wire of the first spark chamber must be added. The angular measuring accuracy of the spark chambers plus the uncertainty in the incident beam angle was 3 mrad FWHM. The ms calculations are based on the work of R. Diebold, SLAC Report No. RD-11, 1967 (unpublished).

¹¹The total "high-resolution" data in Ref. 1, Fig. 4, are compiled from samples with resolutions of 26, 18, and 16 MeV. We estimate the effective resolution of this sample to be 20 MeV FWHM.

¹²C. T. Coffin *et al.*, Phys. Rev. **159**, 1169 (1967).

¹³The fluctuation in the 5-GeV (π^-) data [Fig. 2(a)] just

below $M=1.300$ GeV has been investigated by rebinning these data with the bin origins shifted by 2.5 MeV. Upon rebinning, the fluctuation becomes significantly reduced.

¹⁴The detection efficiencies are calculated assuming a production cross section of the form $d^2\sigma/dMdt = G(M) \times \exp(-B|t-t_M|)$, where $G(M)$ is the total cross section per unit mass for production of particles with an effective mass M , and t_M is the minimum t possible for mass M . The value of $B=8$ GeV⁻², which represents well the t dependence of all the data for $1.1 \leq M \leq 1.5$ GeV, was used in the calculations.

¹⁵A special selection of our 7-GeV data was also made to more closely approximate the exact conditions of the CMMS experiment. For this selection, data were chosen in which one, two, or three charged particles were detected in the hodoscope covering a large portion of the solid angle in the forward direction. Fits to these data favor a Breit-Wigner shape by ~ 12 standard deviations (linear background).

Experimental Limits on the Decays $K_L^0 \rightarrow \mu^+ \mu^-$, $e^+ e^-$, and $\mu^\pm e^\mp$

Alan R. Clark, T. Elioff,* R. C. Field, H. J. Frisch, Rolland P. Johnson,
Leroy T. Kerth, and W. A. Wenzel

Lawrence Radiation Laboratory, University of California, Berkeley, California

(Received 9 April 1971)

We have performed a search at the Bevatron for the decays $K_L^0 \rightarrow \mu^+ \mu^-$, $e^+ e^-$, and $\mu^\pm e^\mp$ with a double magnetic spectrometer using wire spark chambers. Over 10^6 observed $K_L^0 \rightarrow \pi^+ \pi^-$ decays determine the normalization for the di-lepton decay modes. No $e^+ e^-$ or $\mu^\pm e^\mp$ events were observed. For each of these decays the upper limit on the branching ratio relative to all modes is 1.57×10^{-9} (90% confidence level). For the decay $K_L^0 \rightarrow \mu^+ \mu^-$, the limit is 1.82×10^{-9} (90% confidence level).

The $K_L^0 \rightarrow \mu^+ \mu^-$ decay is generally considered to be a sensitive test of the existence of weak neutral currents. This decay should also occur via higher-order weak interactions.¹ Current algebra techniques have been used to relate the rates for $K^+ \rightarrow \mu^+ \nu$ and the second-order weak process $K_L^0 \rightarrow \mu^+ \mu^-$.² An upper bound on the weak interaction cutoff then follows from the experimental limit on $K_L^0 \rightarrow \mu^+ \mu^-$.

The $K_L^0 \rightarrow l^+ l^-$ decays should also be induced by electromagnetic interactions.³ Using the measured $K_L^0 \rightarrow \gamma \gamma$ rate⁴ and assuming only the two-photon intermediate state, branching ratios of approximately 10^{-8} have been predicted from various models for the $K_L^0 \rightarrow \mu^+ \mu^-$ decay.⁵ Neglecting the contributions from off-mass-shell photons, one can derive a "unitarity" lower limit of 6×10^{-9} for this decay. However, other intermediate states may destructively interfere, producing a limit lower than that predicted by the two-photon

state alone. Martin, de Rafael, and Smith⁶ have estimated that contributions from the $\pi\pi\gamma$ and 3π intermediate states can lower the rate by at most 20%.

The $K_L^0 \rightarrow e^+ e^-$ rate is suppressed by a factor of $(m_e/m_\mu)^2$ relative to the $K_L^0 \rightarrow \mu^+ \mu^-$ rate in weak models which use $V-A$ and also in electromagnetic models. The $K_L^0 \rightarrow e^\pm \mu^\mp$ rates are not predictable from any known interaction. Limits on these decays (which violate separate lepton-number conservation) can be compared with limits on $\mu^\pm \rightarrow e^\pm \gamma$ or $\mu^\pm \rightarrow e^\pm e^+ e^-$. Table I shows these limits and previously published limits on the various di-lepton decay modes of the K_L^0 .

Figure 1 shows the plan view of the detection apparatus.⁷ The 6-m-long decay volume began 7.6 m from the production target in the Bevatron external proton beam. The 0.8-msr beam yielded $\sim 6 \times 10^5$ K_L^0 's in the momentum range 0.8-3.2 GeV/c for 6×10^{11} protons on the target. The

Table I. Branching ratio limits at 90% confidence level relative to the total decay rate.

Mode	Previous limit	Reference	This experiment
$K_L^0 \rightarrow \mu^+ \mu^-$	$\leq 2.6 \times 10^{-8}$	a	$\leq 1.82 \times 10^{-9}$
$K_L^0 \rightarrow e^+ e^-$	$\leq 1.5 \times 10^{-7}$	b	$\leq 1.57 \times 10^{-9}$
$K_L^0 \rightarrow \mu^+ e^-$	$\leq 3.7 \times 10^{-6}$	c	$\leq 1.57 \times 10^{-9}$
$\mu^+ \rightarrow e^+ \gamma$	$\leq 2.2 \times 10^{-8}$	d	
$\mu^+ \rightarrow e^+ e^+ e^-$	$\leq 6.2 \times 10^{-9}$	e	

^aP. Darriulat, M. I. Ferrero, C. Grosso, M. Holder, J. Pilcher, E. Radermacher, C. Rubbia, M. Scire, A. Staude, and K. Tittel, Phys. Lett. **33B**, 249 (1970).

^bH. Foeth, M. Holder, E. Radermacher, A. Staude, P. Darriulat, J. Deutsch, K. Kleinknecht, C. Rubbia, K. Tittel, M. I. Ferrero, and C. Grosso, Phys. Lett. **30B**, 282 (1969).

^cV. L. Fitch, R. F. Roth, J. Russ, and W. Vernon, Phys. Rev. **164**, 1711 (1967); M. Bott-Bodenhausen, X. deBouard, D. G. Cassel, D. Dekkers, R. Felst, R. Mermod, I. Savin, P. Scharff, M. Vivargent, T. R. Willitts, and K. Winter, Phys. Lett. **24B**, 194 (1967).

^dS. Parker, H. L. Anderson, and C. Rey, Phys. Rev. **133B**, 768 (1964).

^eS. M. Korenchenko, B. F. Kostin, G. V. Micelmacher, K. G. Nekrasov, and V. S. Smirnov, Joint Institute for Nuclear Research Report No. P1-5542, 1970 (unpublished).

first 13% of the data were taken with helium in the decay volume. The decay volume was later evacuated to reduce neutron-induced background. The momenta of the decay secondaries were measured in symmetric spectrometers, each with a 0.9-m x 0.6-m aperture picture-frame magnet and five double-gap magnetostrictive wire spark chambers. The chambers were designed with low mass (5.2×10^{-4} radiation lengths), and the volumes between the spark chambers were filled with helium to reduce Coulomb scattering.

The line integral of each magnetic field, which was uniform to within 1% over 95% of the aperture, was set to correspond to the c.m. momentum of the $K_L^0 \rightarrow \mu^+ \mu^-$ decay. Therefore, independent of kaon momentum, secondaries from

nearly transverse two-body decays emerged from the magnets essentially parallel to the incident kaon direction. Downstream of the last spark chamber on each side of the apparatus, counter hodoscopes *F* and *R* selected trajectories with maximum horizontal divergences of ± 45 mrad from the beam line. A six-counter array *H* was mounted in front of each *F* hodoscope, and a large counter *T* for fast timing was mounted behind each *R* hodoscope.

Electrons were identified in 2.3-m-long Freon Cherenkov counters, which were found to be more than 99.6% efficient during preliminary tests. Muons were identified by range measurements. The range detectors each contained a 1-m-long carbon block followed by seventeen cells

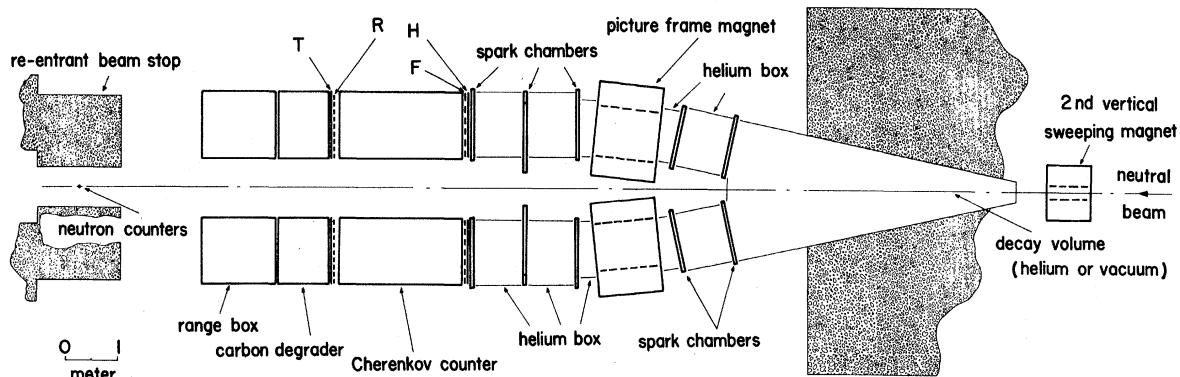


FIG. 1. Plan view of the apparatus. *F* and *R* are counter hodoscopes. *H* is a six-counter array. *T* is a fast-timing counter.

of steel and scintillator. Each cell consisted of one or more 1.2-m \times 1.2-m \times 2.5-cm steel plates and a 1.2-m \times 1.2-m \times 1.9-cm plastic scintillator. The number of iron plates in each cell was chosen to give a muon range interval of approximately 7% for momenta between 0.5 and 1.6 GeV/c.

The trigger logic required a particle on each side which satisfied the angular requirement and also counted in the H array and the timing counter. Events with an electron which bent inward at angles between 15 and 45 mrad were rejected; this veto eliminated a large fraction of the K_{e3} background without affecting the di-lepton acceptance significantly. The signals from the Cherenkov counters (except as noted above) and the range counters were not used in the trigger but were recorded for use later in the analysis. The signals from the counters and the spark-chamber information for each event were accumulated, checked, and then stored on magnetic tape by a model PDP-9 computer. Beam intensity and magnet currents were recorded each Bevatron pulse.

The normalization for the di-lepton decay modes was determined from the simultaneously detected $K_L^0 \rightarrow \pi^+\pi^-$ decays. The acceptance for $K_L^0 \rightarrow \pi^+\pi^-$ relative to that for $K_L^0 \rightarrow \mu^+\mu^-$ was measured to be $(62 \pm 3)\%$. This was done by comparing the rate for detecting $K_L^0 \rightarrow \pi^+\pi^-$ with the magnets set for the $K_L^0 \rightarrow \mu^+\mu^-$ and $K_L^0 \rightarrow \pi^+\pi^-$ c.m. momenta, respectively. The di-pion decay mode also served as a calibration for the invariant-mass scale and a measure of the resolution of the apparatus.

The data were analyzed with a CDC 6600 computer. An event was considered a two-body candidate if the two reconstructed trajectories met within 2 cm in the decay volume and if the reconstructed parent particle originated at a point less than 4.0 cm from the production target. These cuts retained essentially all of the events from $K_L^0 \rightarrow \pi^+\pi^-$ decay. For each two-body candidate with no Cherenkov signals, invariant masses were calculated assuming both particles were either pions or muons. With one Cherenkov count, the event was classed as a $K_L^0 \rightarrow \mu^+e^-$ candidate; with two Cherenkov counts, it was classed as a $K_L^0 \rightarrow e^+e^-$ candidate.

The invariant-mass spectra for $K_L^0 \rightarrow \pi^+\pi^-$ candidates are shown in Figs. 2(a) and 2(b) from data taken with the evacuated decay volume and with helium in the decay volume, respectively. The backgrounds are mostly from $K_L^0 \rightarrow \pi\mu\nu$ decays and from $K_L^0 \rightarrow \pi^+\pi^-$ decays with a pion de-

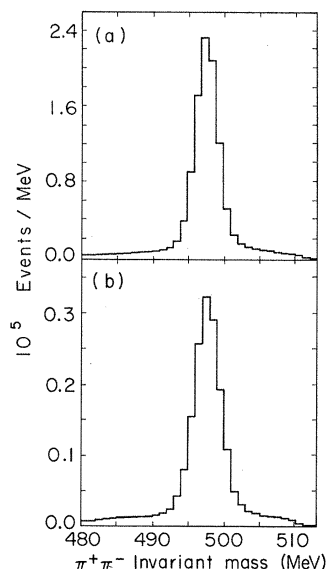


FIG. 2. The di-pion invariant-mass spectra for the data taken with (a) the evacuated decay volume and (b) the helium-filled decay volume. The peak is from the CP -invariance violating decay $K_L^0 \rightarrow \pi^+\pi^-$. The momenta have been reconstructed using an effective-length approximation for the magnetic field. Each reconstructed kaon trajectory is required to pass within 4 cm of the target.

cay in flight. For purposes of normalization these were assumed to contribute flat backgrounds under the $K_L^0 \rightarrow \pi^+\pi^-$ peaks. After subtraction there remain 903 000 $K_L^0 \rightarrow \pi^+\pi^-$ events in the vacuum-data sample and 138 000 in the helium-data sample.

We estimate that 28% of the $K_L^0 \rightarrow \pi^+\pi^-$ events have been lost because of pion decay in flight in the apparatus. After correcting for this loss the effective number of di-pion events in the vacuum- and the helium-data samples are 1 254 000 and 191 700, respectively.

For the analysis above, an effective-length parametrization of the magnetic field was used. This simple procedure, which rejected 98% of the three-body backgrounds, provided good mass resolution for the selection of two-body candidates but inadequate rejection of events in which a secondary pion decayed in flight in the magnet or in which a misidentification of the correct track occurred. Better momentum resolution and discrimination against impossible trajectories were achieved by a step-by-step integration of the trajectories through the measured magnetic fields. The field maps and the integration programs were checked with muon trajectories from $K_{\mu 3}$ decay. A 1.1-MeV invariant-mass resolution

(half width at half-maximum) for the $K_L^0 \rightarrow \pi^+\pi^-$ data was obtained by using the integration procedure.

The secondaries from all $K_L^0 \rightarrow \mu\mu$ candidates with di-muon invariant masses greater than 476 MeV and with measured muon ranges greater than 80% of the predicted muon range were integrated through the magnetic fields. The invariant mass spectra after integration but without any orbit continuity requirements are shown in Figs. 3(a) and 3(b) for the vacuum and helium data, respectively. The sharply falling spectrum at lower invariant masses is the end point from $K_L^0 \rightarrow \pi\mu\nu$ decay with the pion decaying in flight. The flat distribution of events in the helium data appears to be from neutron-helium interactions.

The shaded events in Figs. 3(a) and 3(b) are events which pass an additional cut of four standard deviations on the continuity of the trajectory. The error for each trajectory was calculated by comparing it with approximately 100 muon trajectories with similar topologies from $K_{\mu 3}$ decays. No shaded events are within 5 MeV ($=5\sigma$) of the kaon mass in the vacuum-data sample.

In the helium sample six events remain with invariant mass within 5 MeV of the kaon mass. We have calculated an approximate χ^2 for each of these helium events incorporating the distributions in invariant mass, target position, orbit continuity, and range. The means and standard deviations for these distributions have been determined from the equivalent distributions from the $K_L^0 \rightarrow \pi^+\pi^-$ and $K_L^0 \rightarrow \pi\mu\nu$ events. Of the six events in question, the one with mass of 496.8 has a χ^2 probability of 65% of being compatible with a $K_L^0 \rightarrow \mu^+\mu^-$ decay. The other probabilities in order are 25%, 3%, 2×10^{-4} , $<10^{-4}$, and $<10^{-5}$. We believe this distribution to be caused by neutron-helium interactions. On this basis alone, however, we cannot determine whether or not one of the candidates is a $K_L^0 \rightarrow \mu^+\mu^-$ event.

If one event is interpreted as real, the branching ratio R is determined by the sum of the $K_L^0 \rightarrow \pi^+\pi^-$ events in the helium and the vacuum samples:

$$R = \frac{\Gamma(K_L^0 \rightarrow \mu^+\mu^-)}{\Gamma(K_L^0 \rightarrow \text{all})} = \frac{\Gamma(K_L^0 \rightarrow \pi^+\pi^-) N_{\mu\mu}}{\Gamma(K_L^0 \rightarrow \text{all}) N_{\pi\pi}} A$$

$$= 6.8 \times 10^{-10},$$

where $N_{\mu\mu} = 1$ is the number of observed $K_L^0 \rightarrow \mu^+\mu^-$ events, $N_{\pi\pi}$ is the number of observed $K_L^0 \rightarrow \pi^+\pi^-$ events corrected for losses by decay

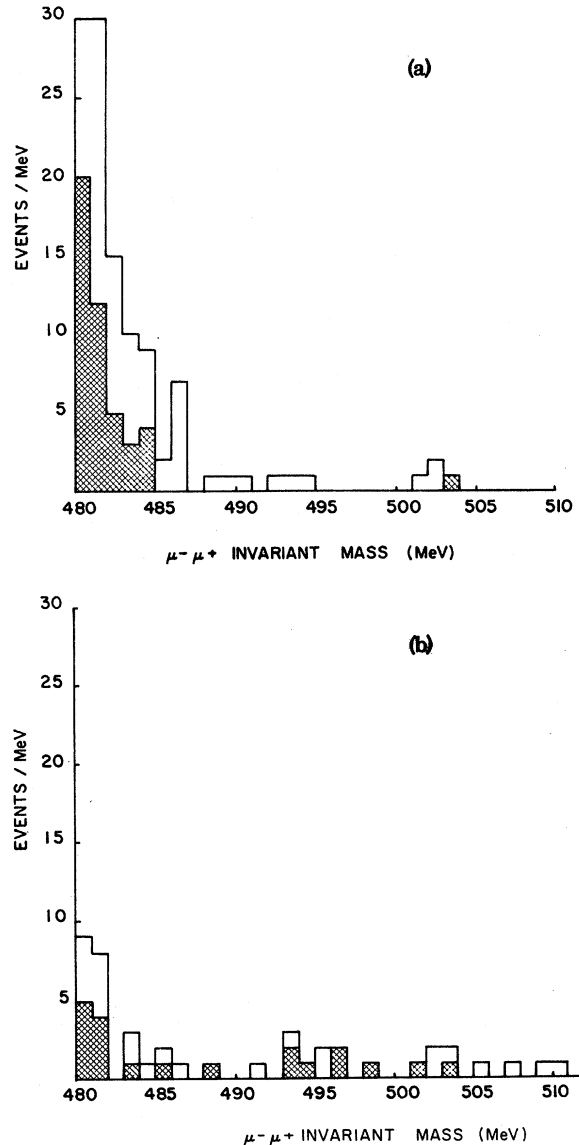


FIG. 3. The di-muon invariant-mass spectra for the data taken with (a) the evacuated decay volume and (b) the helium-filled decay volume. The measured magnetic fields have been used to determine the momenta. Each reconstructed kaon trajectory has been required to pass within 4 cm of the target. Each muon has been required to travel to at least 80% of the expected mean range for its measured momentum. The shaded events have survived a 4σ cut on the orbit continuity in comparison with topologically similar muons from $K_{\mu 3}$ decays.

in flight, and A is the relative acceptance efficiency for $K_L^0 \rightarrow \pi^+\pi^-$ and $K_L^0 \rightarrow \mu^+\mu^-$.

We believe, however, that we can without bias exclude the helium data from consideration because of the backgrounds due to neutron-helium interactions. The vacuum data, 87% of the total

sample, are devoid of candidates. The upper limit on the branching ratio obtained under these clean conditions is

$$R < 1.82 \times 10^{-9} \text{ (90\% confidence level).}$$

The upper limit of 1.82×10^{-9} on the branching ratio for the $K_L^0 \rightarrow \mu^+ \mu^-$ decay is in conflict with the lower "primitive unitarity limit" of 6×10^{-9} . The most uncertain aspect of the unitarity calculation appears to be the contributions from intermediate states other than $\gamma\gamma$. The possible effects of $2\pi\gamma$ and 3π have been estimated by Martin, de Rafael, and Smith.⁶ Their calculation, assuming destructive interference, gives a limit of 4.8×10^{-9} . The probability that the experimental result is in agreement with this bound estimated by Martin, de Rafael, and Smith is approximately 0.3%. We note that if we include the helium data and assume it contains one good event, the probability of agreement is raised to only 0.7%.

The experimental limit from the vacuum data leads to a limit on the weak-interaction cutoff of $\Lambda \leq 19$ GeV based on the intermediate-vector-boson calculations of Ioffe and Shabalin.² With the use of a second-order four-fermion model, their calculation results in a limit of $\Lambda \leq 7$ GeV.

We have performed numerous checks on our apparatus and analysis programs to confirm that we have no bias against di-lepton events. To check the lepton-identification criteria we have compared our measured relative rates for $K_{\pi\pi}$, $K_{\mu 3}$, and $K_{e 3}$ to a Monte Carlo calculation and have found excellent agreement. As has been stated, there is no muon requirement in the trigger. Furthermore, the relative acceptances for $K_L^0 \rightarrow \pi^+ \pi^-$ and $K_L^0 \rightarrow \mu^+ \mu^-$, as measured with the apparatus, agree with the Monte Carlo calculations. Finally we have simulated $K_L^0 \rightarrow \mu^+ \mu^-$

events and analyzed them successfully with the actual reconstruction and analysis programs.

No e^+e^- or $e^+\mu^\mp$ events within 7 MeV of the K mass were observed. The limit from all the data on each of the e^+e^- and $e^+\mu^\mp$ decay modes is

$$\Gamma(K_L^0 \rightarrow l^+ l^-) / \Gamma(K_L^0 \rightarrow \text{all})$$

$$< 1.57 \times 10^{-9} \text{ (90\% confidence level).}$$

We wish to thank the Lawrence Radiation Laboratory engineers, the Bevatron staff, and our technicians for their interest and efforts which made the experiment possible.

†Work done under the auspices of the U. S. Atomic Energy Commission.

*On leave from Lawrence Radiation Laboratory to the U. S. Atomic Energy Commission, Washington, D. C.

¹A. Pais and S. B. Treiman, Phys. Rev. **176**, 1974 (1968).

²B. L. Ioffe and E. P. Shabalin, Yad. Fiz. **6**, 828 (1967) [Sov. J. Nucl. Phys. **6**, 603 (1968)]; R. N. Mohapatra, J. Subba Rao, and R. E. Marshak, Phys. Rev. Lett. **20**, 1081 (1968), and Phys. Rev. **171**, 1502 (1968).

³C. Quigg and J. D. Jackson, UCRL Report No. UCRL-18487, 1968 (unpublished). This article contains an extensive list of references to previous work.

⁴J. E. Enstrom, SLAC Report No. 125, 1970 (unpublished). References to previous $K_L^0 \rightarrow \gamma\gamma$ experiments may be found in this, or in M. Roos, C. Bricman, A. Barbaro-Galtieri, L. R. Price, A. Rittenberg, A. H. Rosenfeld, N. Barash-Schmidt, P. Söding, C. Y. Chien, C. G. Wohl, and T. Lasinski, Phys. Lett. **33B**, 1 (1970).

⁵Quigg and Jackson, Ref. 3, p. 43.

⁶B. R. Martin, E. de Rafael, and J. Smith, Phys. Rev. D **2**, 179 (1970).

⁷A complete description of the apparatus can be found in R. P. Johnson, thesis, UCRL Report No. UCRL-19709, 1970 (unpublished); H. J. Frisch, thesis, UCRL Report No. UCRL-20264, 1971 (unpublished).